Journal of Physiology - Paris 103 (2009) 211–219

Contents lists available at ScienceDirect

Journal of Physiology - Paris

journal homepage: www.elsevier.com/locate/jphysparis

Robotics-based synthesis of human motion

O. Khatib [a,*], E. Demircan [a], V. De Sapio [a,b], L. Sentis [a], T. Besier [c], S. Delp [d]

[a] Artificial Intelligence Laboratory, Stanford University, Stanford, CA 94305, USA
[b] Sandia National Laboratories, Livermore, CA 94551, USA
[c] Human Performance Laboratory, Stanford, CA 94305, USA
[d] Neuromuscular Biomechanics Laboratory, Stanford, CA 94305, USA

ARTICLE INFO

Keywords:
Task-space framework
Human performance characterization
Robotics
Musculoskeletal dynamics
Human animation
Operational space formulation

ABSTRACT

The synthesis of human motion is a complex procedure that involves accurate reconstruction of movement sequences, modeling of musculoskeletal kinematics, dynamics and actuation, and characterization of reliable performance criteria. Many of these processes have much in common with the problems found in robotics research. Task-based methods used in robotics may be leveraged to provide novel musculoskeletal modeling methods and physiologically accurate performance predictions. In this paper, we present (i) a new method for the real-time reconstruction of human motion trajectories using direct marker tracking, (ii) a task-driven muscular effort minimization criterion and (iii) new human performance metrics for dynamic characterization of athletic skills. Dynamic motion reconstruction is achieved through the control of a simulated human model to follow the captured marker trajectories in real-time. The operational space control and real-time simulation provide human dynamics at any configuration of the performance. A new criteria of muscular effort minimization has been introduced to analyze human static postures. Extensive motion capture experiments were conducted to validate the new minimization criterion. Finally, new human performance metrics were introduced to study in details an athletic skill. These metrics include the effort expenditure and the feasible set of operational space accelerations during the performance of the skill. The dynamic characterization takes into account skeletal kinematics as well as muscle routing kinematics and force generating capacities. The developments draw upon an advanced musculoskeletal modeling platform and a task-oriented framework for the effective integration of biomechanics and robotics methods.

1. Introduction

In the field of robotics, the motivation to emulate human movement is driven by the proliferation of humanoid robots and the desire to endow them with human-like movement characteristics (Nakamura et al., 2003). Inspired by human behaviors, our early work in robot control encoded tasks and diverse constraints into artificial potential fields capturing human-like goal-driven behaviors (Khatib and Le Maitre, 1978). This concept was later formalized in the task oriented operational space dynamic framework (Khatib, 1986, 1987). More recently, this formulation was extended to address whole-body control of humanoid robots and successfully validated on physical robots (Khatib et al., 2004). The framework provides multi-task prioritized control architecture allowing the simultaneous execution of multiple objectives in a hierarchical manner, analogous to natural human motion (see Fig. 1).

One of the major difficulties associated with the prediction and synthesis of human movement is redundancy resolution. Whether the goal is to gain an understanding of human motion or to enable synthesis of natural motion in humanoid robots a particularly relevant class of movements involves targeted reaching. Given a specific target the prediction of kinematically redundant limb motion is a problem of choosing one of a multitude of control solutions all of which yield kinematically feasible solutions. It has been observed that humans resolve this redundancy problem in a relatively consistent manner (Kang et al., 2005; Lacquaniti and Soechting, 1982). For this reason, mathematical models have proven to be valuable tools for motor control prediction (Hermens and Gielen, 2004; Vetter et al., 2002). These models frequently characterize some element of musculoskeletal effort.

Robotics-based effort models frequently utilize quantities that are derivable purely from skeletal kinematics and that are not specific to muscle actuation. It is thus useful to consider an analogous measure that encodes information about the overall musculoskeletal system to account for muscle actuation and its redundancy. Activation, which represents the normalized exertion of muscles, provides a natural starting point for constructing such a measure.

* Corresponding author.
E-mail addresses: khatib@cs.stanford.edu (O. Khatib), emeld@cs.stanford.edu (E. Demircan), vdesap@sandia.gov (V. De Sapio), lsentis@cs.stanford.edu (L. Sentis), besier@stanford.edu (T. Besier), delp@stanford.edu (S. Delp).

0928-4257/$ - see front matter © 2009 Elsevier Ltd. All rights reserved.
doi:10.1016/j.jphysparis.2009.08.004

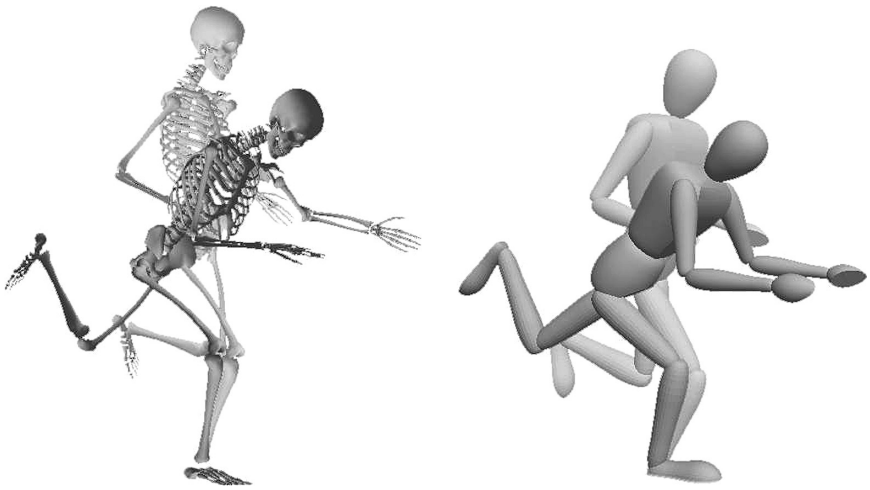

Fig. 1. Task-space framework allows the articulated skeleton to maintain balance while accomplishing a manual task (Khatib et al., 2004).

Specifically, the magnitude of muscle activation vector has been used as an optimization criterion in both static and dynamic optimizations (Thelen et al., 2003). The utilization of a model-based characterization of muscle systems, which accounts for muscle kinematic and strength properties, is critical to authentically simulating human motion since human motions are frequently linked by physiological constraints.

In this paper, a robotic approach for the synthesis of human motion using a task-space framework is presented. For this purpose, the *direct marker control* for human motion reconstruction, a criterion of task-driven *effort minimization* and new metrics for *dynamic characterization* of human performance were introduced. The result is a dynamic biomechanical profile of human performance that facilitates the modeling of human motion. These approaches were tested through extensive motion capture experiments on human subjects including a martial art master and a professional football player. The results showed that these skillful practitioners tend to minimize the muscular effort while following the lines of maximum feasible accelerations when performing a task. These results support our prediction that task-driven human motions emerge from the use of *physiomechanical advantage* of the human musculoskeletal system under physiological constraints.

1.1. Task dynamic behavior and control

For a given desired whole-body task of a human-like robot, the motion behaviors should be specified to be controlled during the execution of the motion. Hand location, balance, effort minimization, and obstacle and joint limit avoidance are common choices, but the exhaustive list depends upon the motion to be performed. Considering each behavior as an independent task, the number of degrees of freedom describing each task is typically less than the number of joints in the robot. For these situations, there are multiple ways of performing the task. This redundancy is labeled in solutions as the posture space of the task, containing all possible motions that do not affect task performance (Khatib et al., 2004). As such, other tasks may be controlled by selectively choosing the path within the posture space.

In this section, the dynamic model of the task/posture decomposition and the model describing the motion of the subtask within the posture space (Khatib et al., 2004) are reviewed. Combination of these two models provides a control structure that compensates for the dynamics in both spaces, significantly improving performance and responsiveness for multiple tasks.

A task can be defined to be any formal description of desired activity that can be explicitly represented as a function of the joint coordinates, q, $\dot{q}$ and $\ddot{q}$. Multiple tasks, x_i's, can be combined into a single task definition in a higher dimensional space, as long as they are kinematically consistent with each other. The task coordinates are denoted by $x_t = x_t(q)$.

The joint space equations of motion can be expressed as,

$$A(q)\ddot{q} + b(q,\dot{q}) + g(q) = \Gamma, \tag{1}$$

where q is the $n \times 1$ vector of generalized coordinates, $A(q)$ is the $n \times n$ mass matrix, $b(q,\dot{q})$ is the $n \times 1$ vector of centrifugal and Coriolis terms, $g(q)$ is the $n \times 1$ vector of gravity terms, and Γ is the $n \times 1$ vector of generalized control forces (torques). For conciseness we will often refrain from explicitly denoting the functional dependence of these quantities on q and $\dot{q}$.

The Jacobian matrix associated with the task, x_t, is denoted by $J_t(q)$. The task dynamic behavior can be obtained by projecting the skeletal dynamics (1) into the space associated with the task, using the generalized inverse of the Jacobian, $\bar{J}_t$. This generalized inverse of the Jacobian has been showed to be unique and dynamically consistent (Khatib, 1987, 1995) and given by,

$$\bar{J}_t \triangleq A^{-1}J_t^T\left(J_tA^{-1}J_t^T\right)^{-1}. \tag{2}$$

The dynamic behavior associated with the task, x_t can be obtained by,

$$\bar{J}_t^T(A\ddot{q} + b + g = \Gamma) \Rightarrow \Lambda_t\ddot{x}_t + \mu_t + p_t = F_t. \tag{3}$$

In this space, Λ_t is the $m \times m$ task inertia matrix, and μ_t, p_t, and F_t are, respectively, the centrifugal and Coriolis forces, gravity effect, and generalized force acting along the direction of the task, x_t.

This process provides a description of the dynamics in task coordinates rather than joint space coordinates (while joint space coordinates are still present in (3), the inertial term involves task space accelerations rather than joint space accelerations).

The control framework defined in terms of the relevant task coordinates, x_t, can be represented using a relevant operational space force, F_t, acting along the same direction. The forces acting along given task coordinates can be mapped to a joint torque, Γ_{task}, by the relationship,

$$\Gamma_{\text{task}} = J_t^TF_t. \tag{4}$$

For a given task, there is a unit inertial behavior, $I_t\ddot{x}_t = F_t^*$ and $I_p\ddot{x}_p = F_p^*$. The nonlinear dynamic control force of the task, F_t, is given by,

$$F_t = \widehat{\Lambda}_t F_t^* + \hat{\mu}_t + \hat{p}_t, \tag{5}$$

where $\widehat{\cdot}$ denotes the estimates of the components of the dynamic models and F^* is the desired force.

The generalized torque/force relationship (Khatib, 1987, 1995) allows for the decomposition of the total torque into two dynamically decoupled torque vectors: the torque corresponding to the commanded task behavior and the torque that only affects posture behaviors in the null space provided by the kinematic redundancy of the musculoskeletal system,

$$\Gamma = \Gamma_{\text{task}} + \Gamma_{\text{posture}}. \tag{6}$$

The operational space formulation determines the torque component for the task to compensate for the dynamics in the task space,

$$\Gamma = \Gamma_{\text{task}} + \Gamma_{\text{posture}} = J_t^T F_t + N_t^T \Gamma_p, \tag{7}$$

where N_t is the null space associated with the task.

Dynamically consistent posture control guarantees posture behaviors to be performed without projecting any acceleration onto the task (Khatib, 1995). Any acceleration associated with the posture that would affect the task is filtered by its null space, N_t.

Postures can be represented by minimal sets of independent posture coordinates,

$$\Gamma_p = J_p^T F_p. \tag{8}$$

The task consistent posture Jacobian $J_{p|t}$ can be defined through the relation,

$$J_{p|t} = J_p N_t. \tag{9}$$

The task description and whole-body dynamic control through prioritization can be obtained by,

$$\overline{J}_{p|t}^T [A\ddot{q} + b + g = \Gamma_{\text{task}} + \Gamma_{\text{posture}}] \Rightarrow \Lambda_{p|t}\ddot{x}_{p|t} + \mu_{p|t} + p_{p|t} = F_{p|t}, \tag{10}$$

and the force/torque relationship,

$$\Gamma_{\text{posture}} = J_{p|t}^T F_{p|t}. \tag{11}$$

Using these dynamic behavior models, a dynamically decoupled control to perform both tasks can be formulated. The control force for the decoupled system, $F_{p|t}$, is given by,

$$F_{p|t} = \widehat{\Lambda}_{p|t} F_{p|t}^* + \hat{\mu}_{p|t} + \hat{p}_{p|t}, \tag{12}$$

where $F_{p|t}^*$ is the desired force for the decoupled system.

Using the task-dependent torque decomposition and the force/torque relationship, the resulting control torque, Γ, is,

$$\Gamma = \Gamma_{\text{task}} + \Gamma_{\text{posture}} = J_t^T F_t + J_{p|t}^T F_{p|t}. \tag{13}$$

The task can be controlled by a task field U_t that determines the desired behavior by its gradient $F_t^* = -\nabla_{x_t} U_t$. Similarly, the posture behavior F_p^* can be specified by a posture field U_t. In the study of human motion, the strategies humans follow to perform skills can be expressed by these energy potentials.

1.2. Human motion reconstruction by direct marker control

The motion capture is an effective tool to investigate human kinematics in a given motion. However, a number of post processing steps need to be performed to convert the raw marker positions into useful kinematic data. The most significant step is to convert the marker trajectories, x, $\dot{x}$ and $\ddot{x}$, into joint space trajectories, q, $\dot{q}$ and $\ddot{q}$. This hascommonly been done using inverse kinematic techniques and an efficient motion analysis requires also solving for human dynamics.

Recently, using the task-oriented control framework we proposed a new approach to reconstruct human movement in real-time through direct control of optical marker trajectory data (Demircan et al., 2008), what we term as *direct marker control*. The direct marker control is achieved by mapping a scaled dynamic human model to the experimental marker locations in Cartesian space and simulating it along the desired trajectories in real-time. In order to accurately reconstruct human motion, the direct marker control algorithm solves the problem of redundancy in having much marker position data than needed to resolve the joint angles and ensures marker decoupling.

The markers mounted on the same body link are rigidly constrained to each other and the relative motion between markers on adjacent links is limited by the freedom in the connecting joints. In order to solve the motion dependencies, we group the markers into independent sets and form a hierarchy of tasks associated with each set. In this *marker space*, a priority is assigned to each task and the tasks that have lower priorities in the hierarchy are projected into the null space of the tasks that have higher priorities. This process is recursively iterated and the human model is tracked to the desired motion configurations.

In order to have kinematically consistent motion patterns, the human model is scaled to the subject's anthropometry. Kinematically correct human model is then simulated in real-time to generate the motion dynamics at any state of the performance. The direct marker control algorithm constitutes an effective tool by extending our dynamic environment to identify the characteristics describing natural human motion which can be mapped into humanoid robots for real-time control and analysis.

1.2.1. Direct marker control framework

The task/posture decomposition used in the operational space method provides an effective method that allows us to represent the dynamics of a simulated human subject in a relevant task space that is complemented by a posture space (7). For an arbitrary number of tasks, the torque decomposition (13) can be generalized to,

$$\Gamma = J_{t_1}^T F_{t_1} + J_{t_2|t_1}^T F_{t_2|t_1} + \cdots + J_{t_n|t_{n-1}|\cdots|t_1}^T F_{t_n|t_{n-1}|\cdots|t_1}. \tag{14}$$

In our direct marker control framework, task space is defined as the space of Cartesian coordinates for the motion capture markers. However, the dependency between marker descriptions is a problem. To accommodate for the marker coupling, we start by selecting an independent set, m_1, of markers and a task, x_{m_1}, associated with this set. The control of the remaining markers is achieved in a manner consistent with the first set by projecting the associated control in the null space of m_1. We continue this process recursively in order to control the remaining markers without interfering with each other and we build a hierarchy of decoupled marker tasks, $x_{m_1}, \ldots, x_{m_n}$, where x_{m_i} denotes the task for a particular marker set, m_i. The overall control torque defined in marker space is then,

$$\Gamma = J_{m_1}^T F_{m_1} + J_{m_2|m_1}^T F_{m_2|m_1} + \cdots + J_{m_n|m_{n-1}|\cdots|m_1}^T F_{m_n|m_{n-1}|\cdots|m_1}. \tag{15}$$

The Jacobian and the force associated with marker space are deduced from the above equation as follows,

$$J_\otimes \triangleq \begin{bmatrix} J_{m_1} \\ J_{m_2|m_1} \\ \vdots \\ J_{m_n|m_{n-1}|\cdots|m_1} \end{bmatrix} \quad \text{and} \quad F_\otimes \triangleq \begin{bmatrix} F_{m_1} \\ F_{m_2|m_1} \\ \vdots \\ F_{m_n|m_{n-1}|\cdots|m_1} \end{bmatrix}. \tag{16}$$

So, Eq. (15) can be written as,

$$\Gamma = J_\otimes^T F_\otimes. \tag{17}$$

1.2.2. Experimental validation

To test the direct marker control algorithm, a series of movements performed by a tai chi master were captured using an 8-camera motion capture system. The motion was then reconstructed in the control and simulation framework, SAI (Khatib et al., 2002) by tracking the marker trajectories in real-time. Prior to tracking, our existing human model which consists of 25 joints, was first scaled to match the anthropometry of the tai chi master. The human motion reconstruction was then executed using sets of decoupled marker trajectories. Fig. 2 illustrates the scaled musculoskeletal model together with the marker sets selected for direct control.

The commanded and tracked positions of the controlled markers (Fig. 3), as well as the joint angles (Fig. 4), were recorded during real-time simulation. The results demonstrated the effectiveness of the direct marker control algorithm in ensuring smooth tracking of marker trajectories and for the extraction of joint angles without inverse kinematics computations.

An analysis on the bounds of the joint space errors can be performed using the Jacobian associated with the marker space, by:

$$\Delta x_{\otimes} = J_{\otimes} \Delta q. \tag{18}$$

Fig. 5 shows the margin of marker position errors and the margin of joint angle errors, respectively. Maximum and minimum joint angle error magnitudes vary stably over the trajectory, suggesting well bounded errors on the joint angles.

2. Human muscular effort characterization

The ability of humans to move and coordinate their limbs in the performance of common tasks is remarkable. When holding a heavy object or applying a force to the environment through a tool, the arms and body of a skillful human are configured in the most effective fashion for the task. The human selection of specific postures among the infinity of possibilities is the result of a long and complex process of learning. Through learning, humans seem to come to discover the properties of their bodies and how best to put them to use when performing a task. Exploiting the body kinematic characteristics, humans are effectively using the body mechanical advantage to improve the transmission of the tension of muscles into task required forces. However, the efficiency of this transmission is also affected by the human muscle actuation physiology. By also adjusting the body configurations to maximize this transmission of muscle tensions to resulting task forces, humans are in fact exploiting what can be termed the *physiomechanical advantage* of their musculoskeletal system. If confirmed, this would corresponds simply to the overall minimization of the human muscular effort.

Consider a limb with one muscle and let m designate the force generated by this muscle. The potential energy, E, associated with the effort minimization can be expressed in the form,

$$E = cm^2, \tag{19}$$

where c is a weighting coefficient used to account for the muscle force generating capacity, when adding the effects of other muscles.

For a multi-muscle musculoskeletal system, the muscular forces take the form of a vector. The corresponding joint torque associated with m is given by the relationship,

$$\Gamma = L^T(q)m, \tag{20}$$

where L is the $r \times n$ muscle Jacobian matrix (moment arms) for a system of n joints and r muscles.

As a criteria for natural human motion, the human posture is continuously adjusted to reduce muscular effort (Khatib et al., 2004). For a given task, the muscle effort measure, $E(q)$, can be given by the constituent terms using the generalized operational space force, F, and the relationship (4), as,

$$E(q) = F^T J(q) \left(L^T(q) N_c^2 L(q) \right)^{-1} J^T(q) F, \tag{21}$$

where N_c is the $r \times r$ muscle capacity matrix and satisfies the relation $c = N_c^{-2}$.

In (21) the terms inside the parentheses reflect the role of muscle physiology including the muscle moment arms and force generating capacities, while the Jacobian, J, reflects the kinematics. In dynamic skills, the inertial forces can be part of the effort measure (21) and are taken into account.

For posture-based analysis the static form of the instantaneous muscle effort measure can be constructed by noting that overall torque is reduced to g, and (21) takes the form as,

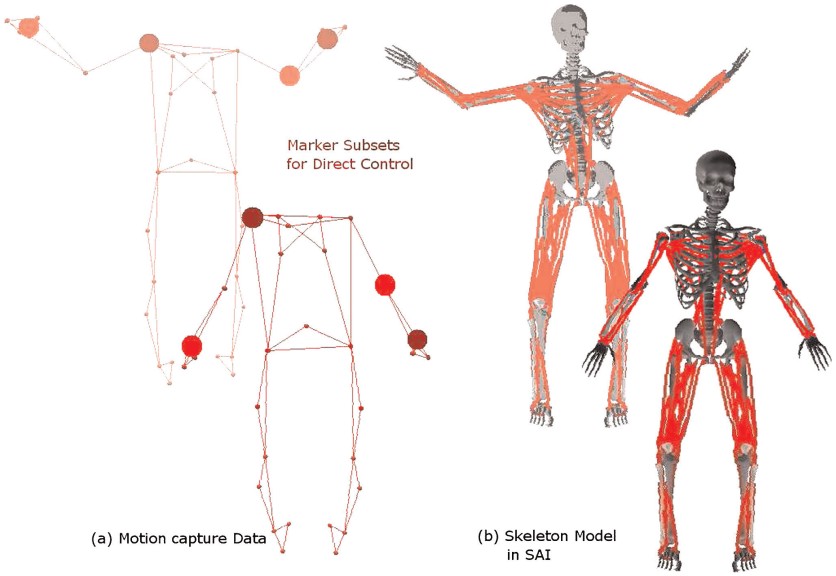

Fig. 2. Scaled human model of a tai chi master. Markers of the right shoulder and the left wrist are selected to form the first marker set to be controlled (dark spheres). The second set is formed by the left elbow and the right wrist markers (light spheres) (Demircan et al., 2008). The musculoskeletal model was derived from models of the upper extremity (Holzbaur et al., 2005) and lower extremity (Delp et al., 1990).

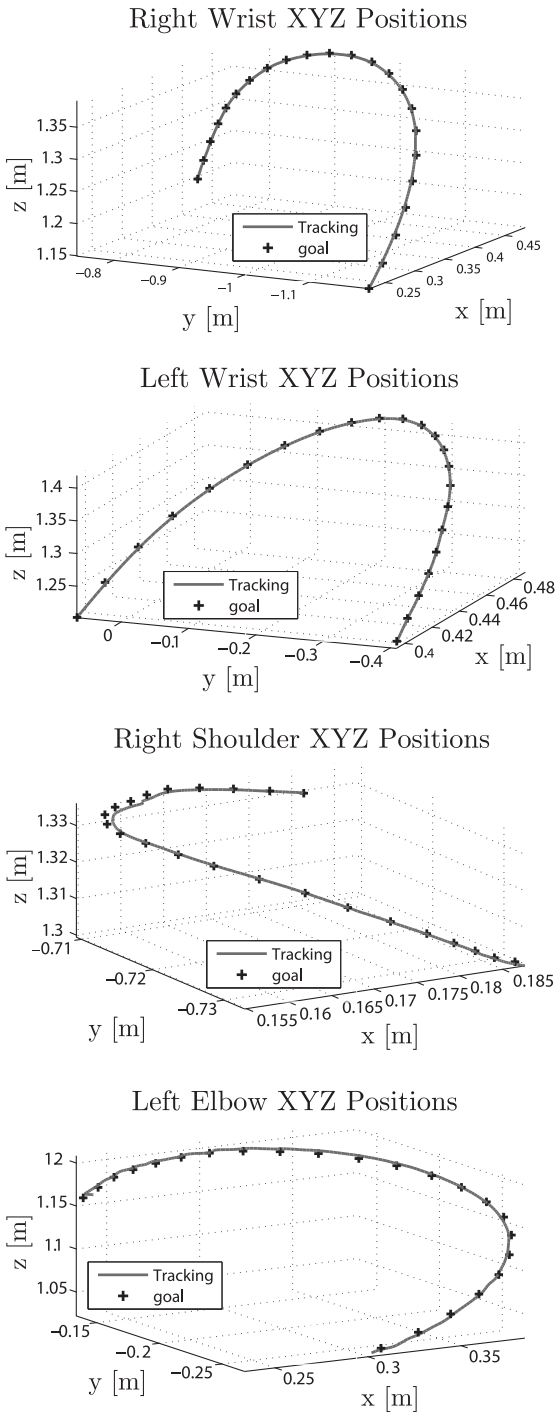

Fig. 3. Tracked and goal trajectories of markers. The tracked trajectories (solid lines) are shown for markers attached to the wrist, shoulder, and elbow segments. The tracked trajectories closely match the goal (experimental) trajectories (dotted crosses) (Demircan et al., 2008).

$$E(q) = g^T(q)\left(L^T(q)N_c^2L(q)\right)^{-1}g(q). \tag{22}$$

2.1. Human musculoskeletal model

In order to evaluate the posture-based muscle effort criterion, a musculoskeletal model must be implemented. Fidelity in predicting muscle lines of action and moment arms was an important requirement for this model. In particular, proper kinematics of

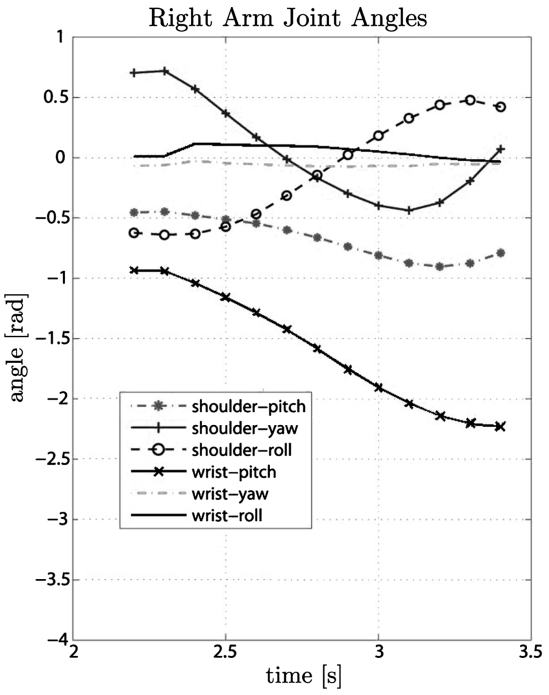

Fig. 4. Right arm joint angles obtained through direct control of marker data. Smooth joint space trajectories are obtained as a natural output of the marker tracking methodology (Demircan et al., 2008).

the shoulder complex are critical in generating realistic muscle paths and associated joint moments of the upper limb. For this reason the upper extremity model of (Holzbaur et al., 2005) has been employed, with some modification, in this work. This model is characterized by coupled motion between the shoulder girdle and the glenohumeral joint. An extensive analysis of this model, in particular the impact of shoulder girdle motion on the muscle routing kinematics and moment arms about the glenohumeral joint, is provided in (De Sapio et al., 2006).

The model, consisting of a constrained shoulder complex and a lower arm, was implemented in the SIMM environment (Delp and Loan, 1995). A minimal set of seven generalized coordinates were chosen to describe the configuration of the shoulder complex (3), elbow (1), and wrist (3). A set of 50 musculotendon units were defined to span each arm (Holzbaur et al., 2005). The kinematic parametrization and musculotendon paths are depicted in Fig. 6.

2.2. Experimental validation

A set of motion capture experiments were conducted with subjects performing static tasks designed to isolate upper limb reaching motion. While seated each subject was instructed to pick up a weight and move it to five different targets and hold a static configuration at each target for 4 s. The posture-based muscle effort criterion (22) was then computed. SIMM was used to generate the maximum muscle induced moments. The results of this analysis showed that the subject's chosen configuration was typically within several degrees of the predicted configuration associated with minimizing the computed muscle effort (De Sapio et al., 2006). Fig. 7 depicts the results of the muscle effort computations for one of the subject trials with no weight in hand.

3. Performance characteristics in human dynamic motion

This section introduces an extended methodology for identifying physiological characteristics that shape human movement.

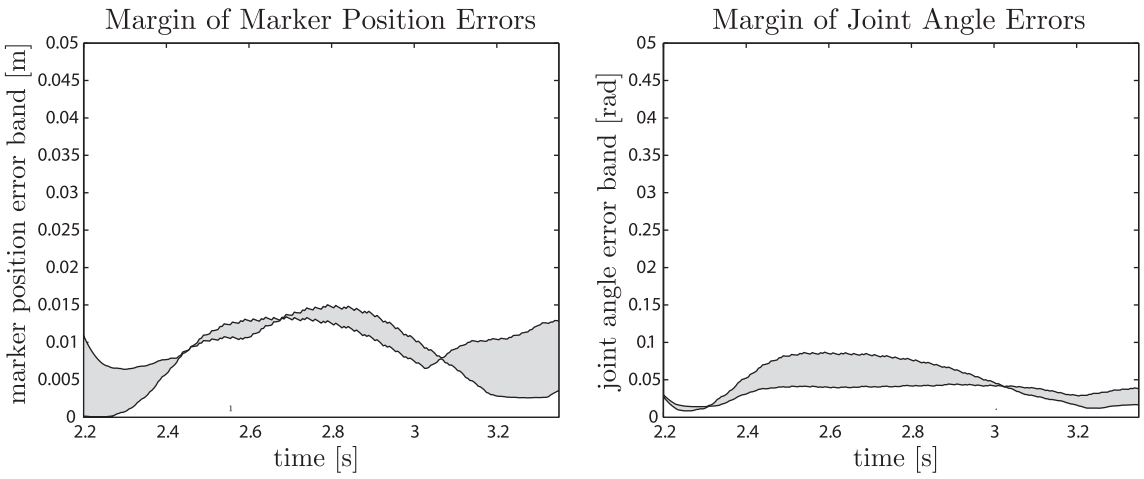

Fig. 5. Margin of marker position errors and margin of joint angle errors over the trajectory. Joint angle error magnitudes show a stable variation over the trajectory, thus ensuring well bounded errors on the joint angles (Demircan et al., 2008).

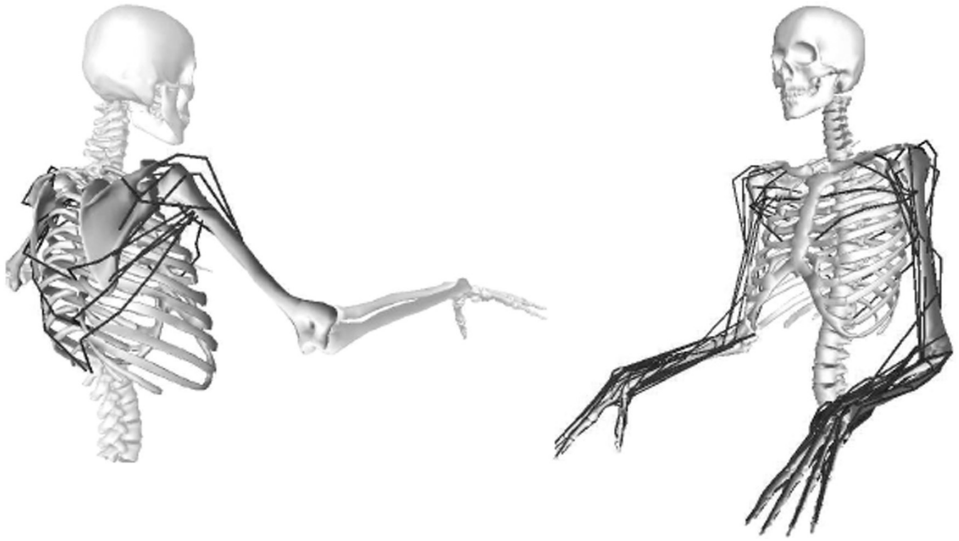

Fig. 6. Kinematic parametrization of the upper extremity model. (Left) A set of seven generalized coordinates were chosen to describe the configuration of the shoulder complex (3), elbow (1), and wrist (3). (Right) A set of 50 musculotendon units were defined to span each arm (Holzbaur et al., 2005).

For this purpose, previously explained human effort minimization strategy (21) was generalized for dynamic skills. As an example illustrating a dynamic skill, we characterized the throwing motion of a football player. In our approach, the performance that suits the footballer can be defined as the ability to achieve maximal ball velocity given the physiological constraints of the system (i.e. limb length, joint range of motion, and muscle strength and contraction velocity). The physiological constraints that affect human motion include the joint constraints (the range of motion at a joint), the segment constraints (the lengths of each segment) and the muscle constraints including physiological cross-section of a muscle, maximum contraction velocity, moment arm and line of action. The football throwing motion was recorded using an 8-camera Vicon motion capture system (OMG plc, Oxford UK) at a capture rate of 120 Hz and the simulation was generated in OpenSim (Delp et al., 2007) and SAI (Khatib et al., 2002) frameworks for the analysis.

In order to investigate the muscular effort in dynamic skills in terms of the musculoskeletal parameters, Eq. (21) can be written in the form,

$$E = F^T \Phi(q) F, \tag{23}$$

where F represents the task requirements and,

$$\Phi(q) \triangleq J\left(L^T(q) N_c^2 L(q)\right)^{-1} J^T. \tag{24}$$

Here, the function $\Phi(q)$ captures the spacial characterization of the muscular effort measure by connecting the muscle physiology to the resulting task, F, through the Jacobian, J.

We studied the dynamic performance characterization and used a graphical representation of the muscular effort function (24) by computing its eigenvalue and eigenvector at a given configuration. The ellipsoids corresponding to the muscular effort were calculated in SAI using the ellipsoid expansion model (Khatib and Burdick, 1987). Results of this analysis showed that the direction of the function (24) was minimized in space, which was equivalent to the minimization of the instantaneous effort in the performance of the throwing skill. Fig. 8 shows the ellipsoids corresponding to task-based muscle effort calculations for selected five configurations.

The current approach involves scaling a musculoskeletal model to match an individuals' anthropometry and provide subject-specific muscle-tendon and joint parameters, such as; muscle-tendon lengths, moment arms, lines of action, and joint topology. As such,

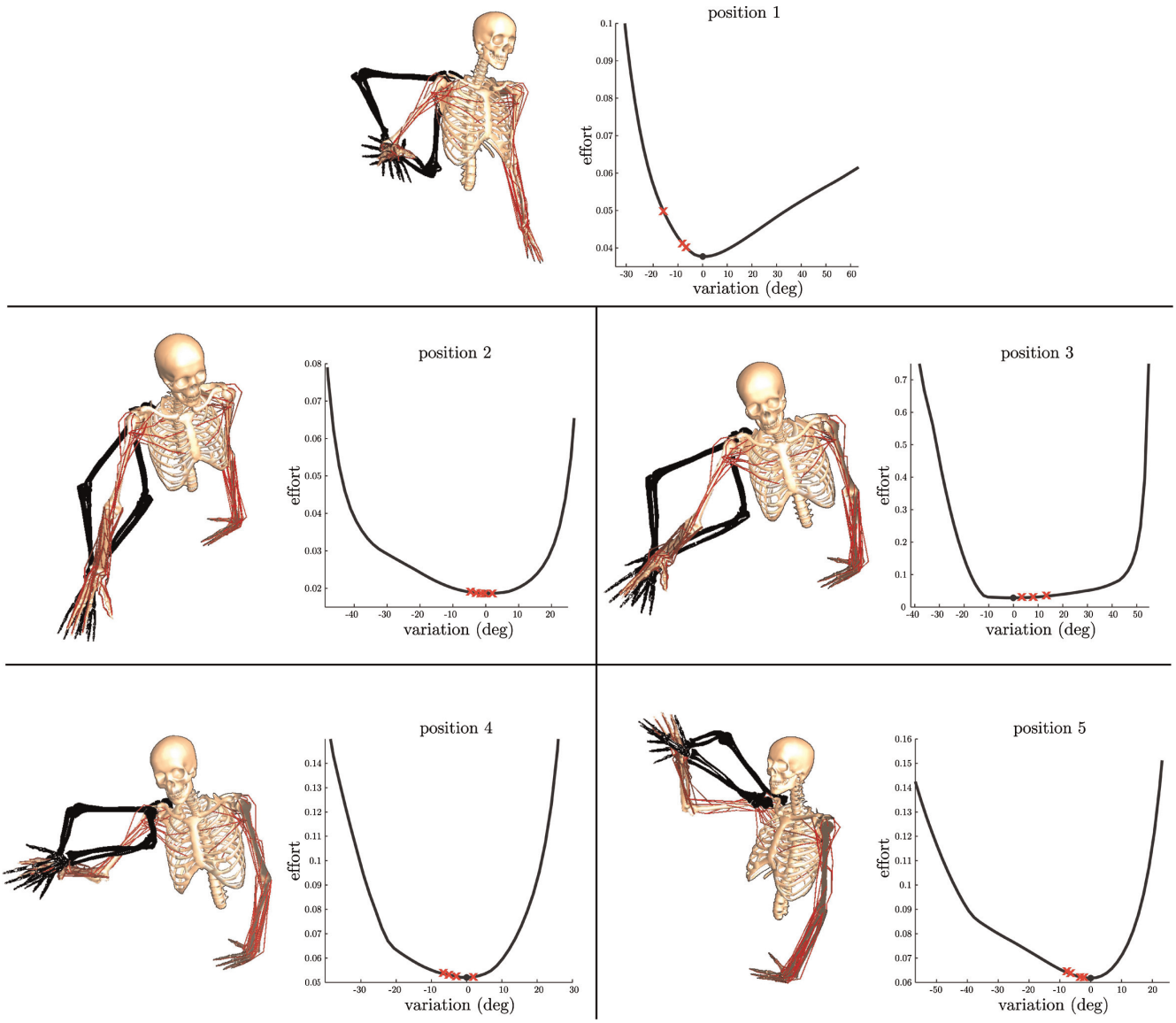

Fig. 7. Muscle effort variation for one of the subject trials with no weight in hand. Each plot depicts the muscle effort for one of the five target configurations. The locations of the subject's chosen configurations are depicted with a "+". The full range of motion is depicted by the black silhouettes (±90 from nominal) (De Sapio et al., 2006).

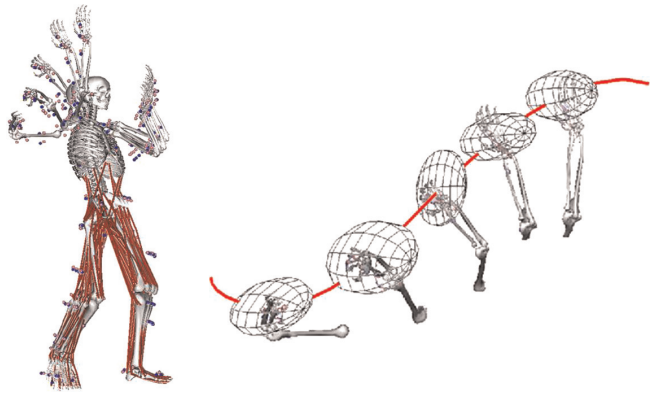

Fig. 8. Task-based analysis of muscular effort. The muscle effort variation for selected five configurations during a football throwing motion represented by ellipsoid expansion model (Khatib and Burdick, 1987). The throwing hand trajectory follows the direction of the ellipsoid associated with the minimum instantaneous effort.

this technique inherently accounts for differences between individuals due to changes in body size. The technique would, therefore, predict that subjects of different stature would perform the same task (i.e. maximum velocity throwing) with slightly different joint kinematics.

Dynamic characterization of human performance needs also to include the analysis of the operational space accelerations. This is motivated by the successful extension of operational space control to analyze the dynamic performance of robotic systems (Khatib and Burdick, 1987). In this framework, the idea is to map the analysis of bounds on joint torques to the resulting end-effector accelerations in the workspace of the manipulator (see Fig. 9). Similar model can be applied to characterize and analyze human dynamic skills shaped by the skeletal mechanics as well as the physiological parameters.

For this system of n equations and r muscles, Γ is the $r \times 1$ vector of muscle induced joint torques and A is the $n \times n$ mass matrix. Using the operational space acceleration/muscle force relationship,

$$\ddot{x} = J(q)A^{-1}(q)(\Gamma - b(q,\dot{q}) - g(q)), \tag{25}$$

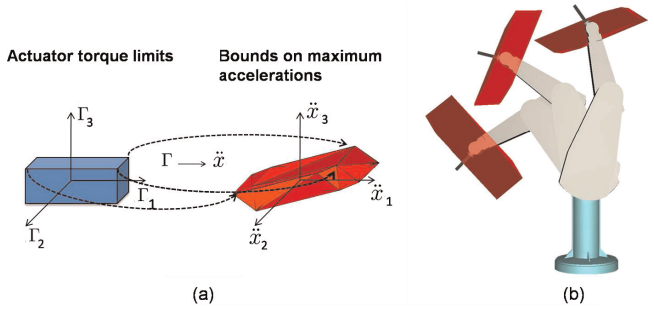

Fig. 9. (a) The bounds on the joint torques of a multi-degrees of freedom manipulator are mapped to the bounds on the resulting accelerations to evaluate its dynamic behavior (Khatib and Burdick, 1987). (b) The acceleration boundaries of the wrist of a 6 degree of freedom robotic system: Puma 560. The 3-D parallelepipeds represent the feasible sets of operational space accelerations for different end-effector configurations.

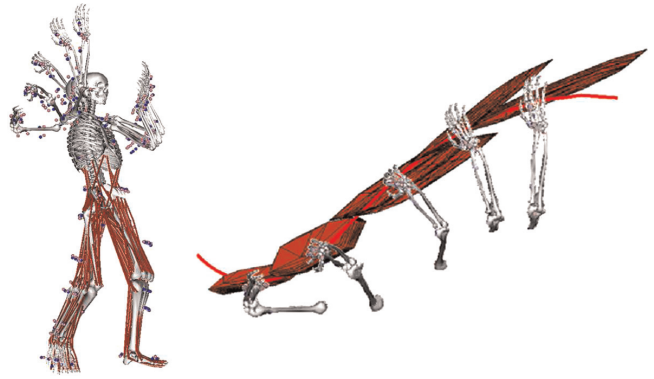

Fig. 10. The feasible set of operational space accelerations bounded by the subject's physiological constraints for selected five configurations of a football throwing motion. Accelerations of the throwing hand can be used for the performance characterization of human dynamic skills.

where $b(q,\dot{q})$ and $g(q)$ are, respectively, the centrifugal and Coriolis torque vector and the gravity torque vector.

The feasible range of accelerations can be determined using (25) given the bounds on the muscle induced torque capacities by,

$$0 < \Gamma < L^T(q) m_{max}. \tag{26}$$

The musculoskeletal model was implemented in SAI control and simulation environment (Khatib et al., 2002) which provided the position Jacobian, J, the muscle Jacobian, L, as well as the muscle induced torques capacities, Γ, and the feasible set of operational accelerations, $\ddot{x}$, for a given configuration, q.

The bounds on the feasible set of acceleration were calculated by the convex hull of the affine transformation of a hypercube for r muscles. The hypercube describing the set of allowable muscle induced torques has 2^r vertices. Fig. 10 illustrates the feasible set of accelerations produced by 12 muscles that contributed most to the resulting acceleration of the hand for selected five configurations.

4. Discussion

A robotics-based approach for the synthesis of human motion using task-level control was presented. Concurrent tools in biomechanics and robotics communities enabled our effort to explore natural human motion having benefits in rehabilitation and facilitating development of human-inspired robots. For this purpose, our existing robotic tools were applied to reconstruct and analyze human skills, introducing the approaches of direct marker control, muscle effort criteria and dynamic characterization of human performance.

For human motion reconstruction, an extension of operational space control (Khatib, 1987) to account for the marker space from human motion capture was presented. The direct marker control algorithm was tested by reconstructing a sequence of motions of a tai chi master and extracting the joint angles in real-time. This algorithm which currently assumes rigid body dynamics will be extended to account for elastic body links in order to better match subject specific anthropometry.

For muscular effort minimization, a new posture-based muscle effort criterion was implemented. This criterion is a generalization of the joint decoupled measure used previously (Khatib et al., 2004). The new criterion properly accounts for the cross-joint coupling associated with multi-articular muscle routing kinematics. Through a set of subject trials good correlation between natural reaching postures and those predicted by our posture-based muscle effort criterion were shown.

What distinguishes our muscle effort criterion is not its implementation as a posture-based or trajectory-based model, since it is amenable to both, but that it characterizes effort expenditure in terms of musculoskeletal parameters, rather than just skeletal parameters. For the characterization of effort expenditure in terms of both skeletal parameters and the muscle physiology, the muscle effort criterion was implemented to analyze a throwing motion of a football player. The results showed that during the performance of the motion the subject tends to minimize the muscular effort defined by the combination of the force generating kinetics of the muscles as well as the mechanical advantage, as determined by the muscle routing kinematics and limb mechanics. Additionally, available set of the operational space accelerations of the throwing hand were used to support the characterization of the same dynamic skill.

One might expect localized muscle fatigue or differences in muscle strength to alter movement patterns when performing the same task. Muscle fatigue, atrophy, or strength can be simulated within our muscular effort criteria by altering the muscle parameters within the model (muscle capacity, c). In the case of fatigue, for example, the force producing capacity of a muscle group can be altered, and the generalized approach would predict a slightly different movement trajectory to compensate for this reduced capacity. As such, the methods presented are generalized and not limited solely to optimal movements.

Accurate modeling and detailed understanding of human motion will have a significant impact on a host of domains: from the rehabilitation of patients with physical impairments to the training of athletes or the design of machines for physical therapy and sport. In the case of rehabilitation, a patient would benefit from knowing what movement pattern might influence loads on a specific joint or tissue. For example, a patient who has undergone arthroscopic knee meniscectomy is at high risk of developing knee joint osteoarthritis, particularly if they walk with large knee adduction (varus) moments. In this scenario, the patient would benefit from knowing what movement pattern could be used to reduce loading on the medial compartment of the knee during walking, thus alleviating the stresses on the articular surface of the knee and reducing the risk of developing osteoarthritis. An additional term describing the loads at the knee could easily be added to the current optimization criteria and the generalized robotics technique could be used to predict a novel gait pattern for the patient that minimizes energy expenditure during walking as well as reducing the loads on the knee. The patient would then be taught this new gait pattern using visual or haptic feedback. This scenario is currently being investigated by the authors.

In spite of the great complexity of natural human motion, the robotic-based analysis of human performance provides substantial

benefits to researchers focused on restoring or improving human movement. Human motor performance depends on skilled motor coordination as well as physical strength. Optimal movements such as those exhibited by highly skilled practitioners in sports and the martial arts provide inspiration for developers of humanoid robots. This dual dependency motivates our work on the analysis and synthesis of human motion.

Acknowledgements

The financial support of the Simbios National Center for Biomedical Computing Grant (http://simbios.stanford.edu/, NIH GM072970), Honda Company and KAUST (King Abdullah University of Science and Technology) are gratefully acknowledged. Many thanks to Francois Conti and Jinsung Kwong for their valuable contributions to the preparation of this manuscript.

References

De Sapio, V., Warren, J., Khatib, O., 2006. Predicting reaching postures using a kinematically constrained shoulder model. In: Lenarcic, J., Roth, B. (Eds.), Advances in Robot Kinematics. Springer, pp. 209–218.

Delp, S.L., Loan, J.P., Hoy, M.G., Zajac, F.E., Topp, E.L., Rosen, J.M., 1990. An interactive graphics-based model of the lower extremity to study orthopaedic surgical procedures. IEEE Transactions on Biomedical Engineering 37, 757–767.

Delp, S., Loan, P., 1995. A software system to develop and analyse models of musculoskeletal structures. Computers in Biology and Medicine 25, 21–34.

Delp, S.L., Anderson, F.C., Arnold, A.S., Loan, P., Habib, A., John, C.T., Guendelman, E., Thelan, D.G., 2007. OpenSim: open-source software to create and analyze dynamic simulations of movement. IEEE Transactions on Biomedical Engineering 55, 1940–1950.

Demircan, E., Sentis, L., De Sapio, V., Khatib, O., 2008. Human motion reconstruction by direct control of marker trajectories. In: Lenarcic, J., Wenger, P. (Eds.), Advances in Robot Kinematis. Springer, Netherlands, pp. 263–272.

Hermens, F., Gielen, S., 2004. Posture-based or trajectory-based movement planning: a comparison of direct and indirect pointing movements. Experimental Brain Research 159 (3), 340–348.

Holzbaur, K.R., Murray, W.M., Delp, S.L., 2005. A model of the upper extremity for simulating musculoskeletal surgery and analyzing neuromuscular control. Annals of Biomedical Engineering 33 (6), 829–840.

Kang, T., He, J., Helms Tillery, S.I., 2005. Determining natural arm configuration along a reaching trajectory. Experimental Brain Research 167 (3), 352–361.

Khatib, O., Le Maitre, J.F., 1978. Dynamic control of manipulators operating in a complex environment. In: Proceedings RoManSy'78, 3rd CISM-IFToMM Symp. Theory and Practice of Robots and Manipulators, Udine, Italy, pp. 267–282.

Khatib, O., 1986. Real-time obstacle avoidance for manipulators and mobile robots. International Journal of Robotic Research 5 (1), 90–98.

Khatib, O., 1987. A unified approach for motion and force control of robot manipulators: the operational space formulation. International Journal of Robotics and Automation 3 (1), 43–53.

Khatib, O., Burdick, J., 1987. Optimization of dynamics in manipulator design: the operational space formulation. International Journal of Robotics and Automation 2 (2), 90–98.

Khatib, O., 1995. Inertial properties in robotic manipulation: an object level framework. International Journal of Robotics Research 14 (1), 19–36.

Khatib, O., Brock, O., Chang, K., Conti, F., Ruspini, D., Sentis, L., 2002. Robotics and interactive simulation. Communications of the ACM 45 (3), 46–51.

Khatib, O., Sentis, L., Park, J., Warren, J., 2004. Whole-body dynamic behavior and control of human-like robots. International Journal of Humanoid Robotics 1 (1), 29–43.

Khatib, O., Warren, J., De Sapio, V., Sentis, L., 2004. Human-like motion from physiologically-based potential energies. In: Lenarčič, J., Galletti, C. (Eds.), On Advances in Robot Kinematics. Kluwer, pp. 149–163.

Lacquaniti, F., Soechting, J.F., 1982. Coordination of arm and wrist motion during a reaching task. Journal of Neuroscience 2 (4), 399–408.

Nakamura, Y., Yamane, K., Suzuki, I., Fujita, Y., 2003. Dynamic computation of musculo-skeletal human model based on efficient algorithm for closed kinematic chains. In: Proceedings of the 2nd International Symposium on Adaptive Motion of Animals and Machines, Kyoto, Japan, SaP-I-2.

Thelen, D.G., Anderson, F.C., Delp, S.L., 2003. Generating dynamic simulations of movement using computed muscle control. Journal of Biomechanics 36, 321–328.

Vetter, P., Flash, T., Wolpert, D.M., 2002. Planning movements in a simple redundant task. Current Biology 12 (6), 488–491.